

## Chapter 1

### Skyrmion Approach to finite density and temperature

Byung-Yoon Park<sup>1</sup> and Vicente Vento<sup>2</sup>

<sup>1</sup> *Department of Physics, Chungnam National University  
Daejeon 305-764, Korea  
bypark@cnu.ac.kr*

<sup>2</sup> *Departament de Física Teòrica and Institut de Física Corpuscular  
Universitat de València and Consejo Superior de Investigaciones Científicas  
E-46100 Burjassot (València), Spain  
Vicente.Vento@uv.es*

We review an approach, developed over the past few years, to describe hadronic matter at finite density and temperature, whose underlying theoretical framework is the Skyrme model, an effective low energy theory rooted in large  $N_c$  QCD. In this approach matter is described by various crystal structures of skyrmions, classical topological solitons carrying baryon number, from which conventional baryons appear by quantization. Chiral and scale symmetries play a crucial role in the dynamics as described by pion, dilaton and vector meson degrees of freedom. When compressed or heated skyrmion matter describes a rich phase diagram which has strong connections with the confinement/deconfinement phase transition.

#### 1.1. Introduction

An important issue at present is to understand the properties of hadronic matter under extreme conditions, e.g., at high temperature as in relativistic heavy-ion physics and/or at high density as in compact stars. The phase diagram of hadronic matter turns out richer than what has been predicted by perturbative Quantum Chromodynamics (QCD).<sup>1</sup> Two approaches have been developed thus far to discuss this issue : on the one hand, Lattice QCD which deals directly with quark and gluon degrees of freedom, and on the other, effective field theories which are described in terms of hadronic fields. We shall describe in here a formalism for the second approach based on the topological soliton description of hadronic matter firstly introduced by Skyrme.<sup>2,3</sup>

Lattice QCD, the main computational tool accessible to highly nonperturbative QCD, has provided much information on the the finite temperature transition, such as the value of the critical temperature, the type of equation of state, etc.<sup>4</sup>

However, due to a notorious ‘sign problem’, lattice QCD could not be applied to study dense matter. Only in the last few years, it has become possible to simulate QCD with small baryon density.<sup>5</sup> Chiral symmetry is a flavor symmetry of QCD which plays an essential role in hadronic physics. At low temperatures and densities it is spontaneously broken leading to the existence of the pion. Lattice studies seem to imply that chiral symmetry is restored in the high temperature and/or high baryon density phases and that it may go hand-in-hand with the confinement/deconfinement transition. The quark condensate  $\langle \bar{q}q \rangle$  of QCD is an order parameter of this symmetry and decreases to zero when the symmetry is restored.

The Skyrme model, is an effective low energy theory rooted in large  $N_c$  QCD,<sup>6,15</sup> which we have applied to dense and hot matter studies.<sup>7–14</sup> The model does not have explicit quark and gluon degrees of freedom, and therefore one can not investigate the confinement/deconfinement transition directly, but we may study the chiral symmetry restoration transition which occurs close by. The schemes which aim at approaching the phase transition from the hadronic side are labelled ‘bottom up’ schemes. The main ingredient associated with chiral symmetry is the pion, the Goldstone boson associated with the spontaneously broken phase. The various patterns in which the symmetry is realized in QCD will be directly reflected in the in-medium properties of the pion and consequently in the properties of the skyrmions made of it.

The most essential ingredients of the Skyrme model are the pions, Goldstone bosons associated with the spontaneous breakdown of chiral symmetry. Baryons arise as topological solitons of the meson Lagrangian. The pion Lagrangian can be realized non-linearly as  $U = \exp(i\vec{\tau} \cdot \vec{\pi}/f_\pi)$ , which transforms as  $U \rightarrow g_L U g_R^\dagger$  under the global chiral transformations  $SU_L(N_f) \times SU_R(N_f)$ ;  $g_L \in SU_L(N_f)$  and  $g_R \in SU_R(N_f)$ . Hereafter, we will restrict our consideration to  $N_f = 2$ . In the case of  $N_f = 2$ , the meson field  $\pi$  represents three pions as

$$\vec{\tau} \cdot \vec{\pi} = \begin{pmatrix} \pi^0 & \sqrt{2}\pi^+ \\ \sqrt{2}\pi^- & -\pi^0 \end{pmatrix}. \quad (1.1)$$

The Lagrangian for their dynamics can be expanded in powers of the right and left invariant currents  $R_\mu = U \partial_\mu U^\dagger$  and  $L_\mu = U^\dagger \partial_\mu U$ , which transforms as  $R_\mu \rightarrow g_L R_\mu g_L^\dagger$  and  $L_\mu \rightarrow g_R L_\mu g_R^\dagger$ . The lowest order term is

$$\mathcal{L}_\sigma = \frac{f_\pi^2}{4} \text{tr}(\partial_\mu U^\dagger \partial^\mu U). \quad (1.2)$$

Here,  $f_\pi = 93$  MeV is the pion decay constant.

Throughout this paper, we take the following convention for the indices: (i)  $a, b, \dots = 1, 2, 3$  (Euclidean metric) for the isovector fields; (ii)  $i, j, \dots = 1, 2, 3$  (Euclidean metric) for the spatial components of normal vectors; (iii)  $\mu, \nu, \dots = 0, 1, 2, 3$  (Minkowskian metric) for the space-time 4-vectors; (iv)  $\alpha, \beta, \dots = 0, 1, 2, 3$  (Euclidean metric) for isoscalar(0)+ isovectors(1,2,3).

In the next order, one may find three independent terms consistent with Lorentz invariance, parity and  $G$ -parity as

$$\mathcal{L}_4 = \alpha \text{tr}[L_\mu, L_\nu]^2 + \beta \text{tr}\{L_\mu, L_\nu\}_+ + \gamma \text{tr}(\partial_\mu L_\nu)^2. \quad (1.3)$$

In his original work,<sup>2,3</sup> Skyrme introduced only the first term to be denoted as

$$\mathcal{L}_{\text{sk}} = \frac{1}{32e^2} \text{tr}[L_\mu, L_\nu]^2, \quad (1.4)$$

which it is still second order in the time derivatives. The value of the “Skyrme parameter” may be evaluated by using  $\pi\pi$  data. In the Skyrme model, it is also determined, for example, as  $e = 5.45$ <sup>16</sup> to fit the nucleon-Delta masses, or as  $e = 4.75$ <sup>17</sup> to fit the axial coupling constant of nucleon.

One may build up higher order terms with more and more phenomenological parameters. However, this naive derivative expansion leads to a Lagrangian which has an excessive symmetry; that is, it is invariant under  $U \leftrightarrow U^\dagger$ , which is not a genuine symmetry of QCD. To break it, we need the Wess-Zumino-Witten term.<sup>18</sup> The corresponding action can be written locally as

$$S_{WZW} = -\frac{iN_c}{240\pi^2} \int d^5x \varepsilon^{\mu\nu\lambda\rho\sigma} \text{tr}(L_\mu L_\nu \cdots L_\sigma), \quad (1.5)$$

i.e. in a five dimensional space whose boundary is the ordinary space and time. For  $N_f = 2$  this action vanishes trivially, but for  $N_f = 3$  it provides a hypothesized process  $KK \rightarrow \pi^+ \pi^0 \pi^-$ . When the action is  $U(1)$  gauged for the pions to interact with photons, this term plays a nontrivial role even with two flavors.

Chiral symmetry is explicitly broken by the quark masses, which provides the masses to the Goldstone bosons. The mass term can be incorporated in the same way as chiral symmetry is broken in QCD; that is,

$$\mathcal{L}_m = \frac{f_\pi^2 m_\pi^2}{4} \text{tr}((U + U^\dagger - 2)) \sim -\frac{\langle \bar{q}q \rangle}{4} \text{tr}(\mathcal{M}(U + U^\dagger - 2)), \quad (1.6)$$

where

$$\mathcal{M} = \begin{pmatrix} m_u & 0 \\ 0 & m_d \end{pmatrix}. \quad (1.7)$$

We neglect the u- and d-quark mass difference.

The approach has been generalized to more sophisticated meson Lagrangians which are constructed by implementing the symmetries of QCD.<sup>19</sup> The scale dilaton has been incorporated into the effective scheme to describe in hadronic language the scale anomaly.<sup>20,21</sup> The vector mesons  $\rho$  and  $\omega$  with masses  $m_{\rho,\omega} \sim 780$  MeV can be incorporated into the Lagrangian by using the hidden local symmetry (HLS)<sup>22</sup> and guided by the matching of this framework to QCD in what is called ‘vector manifestation’ (VM).<sup>23</sup> We shall discuss these generalizations, when required in the discussion of skyrmion matter, later on.

The classical nature of skyrmions enables us to construct a dense system quite conveniently by putting more and more skyrmions into a given volume. Then,

skyrmions shape and arrange themselves to minimize the energy of the system. The ground state configuration of skyrmion matter are crystals. At low density it is made of well-localized single skyrmions.<sup>24</sup> At a critical density, the system undergoes a structural phase transition to a new kind of crystal. It is made of ‘half-skyrmions’ which are still well-localized but carry only half winding number. In the half-skyrmion phase, the system develops an additional symmetry which leads to a vanishing average value of  $\sigma = \frac{1}{2}\text{Tr}(U)$ , the normalized trace of the  $U$  field.<sup>25</sup> In the studies of the late 80’s,<sup>26</sup> the vanishing of this average value  $\langle\sigma\rangle$  was interpreted as chiral symmetry restoration by assuming that  $\langle\sigma\rangle$  is related to the QCD order parameter  $\langle\bar{q}q\rangle$ . However, in Ref. 7, it was shown that the vanishing of  $\langle\sigma\rangle$  cannot be an indication of a genuine chiral symmetry restoration, because the decay constant of the pion fluctuating in such a half-skyrmion matter does not vanish. This was interpreted as a signal of the appearance of a pseudogap phase similar to what happens in high  $T_c$  superconductors.<sup>27</sup>

The puzzle was solved in Ref. 10 by incorporating a suitable degree of freedom, the dilaton field  $\chi$ , associated to the scale anomaly of QCD. The dilaton field takes over the role of the order parameter for chiral symmetry restoration. As the density of skyrmion matter increases, both  $\langle\sigma\rangle$  and  $\langle\chi\rangle$  vanish (not necessarily at the same critical density). The effective decay constant of the pion fluctuation vanishes only when  $\langle\chi\rangle$  becomes zero. It is thus the dilaton field which provides the mechanism for chiral symmetry restoration.

Contrary to lattice QCD, there are few studies on the temperature dependence of skyrmion matter. Skyrmion matter has been heated up to melt the crystal into a liquid to investigate the crystal-liquid phase transition<sup>28,29</sup> a phenomenon which is irrelevant to the restoration of chiral symmetry. We have studied skyrmion matter at *finite density and temperature* and have obtained the phase diagram describing the realization of the chiral symmetry.<sup>14</sup>

The contents of this review are as follows. Section 1.2 deals with the history of skyrmion matter and how our work follows from previous investigations. We also study of the pion properties inside skyrmion matter at finite density. To confront the results with reality, in Sec. 1.3 we show that the scale dilaton has to be incorporated and we discuss how the properties of the pion change thereafter. Section 1.4 is devoted to the study of the temperature dependence and the description of the phase diagram. In Sec. 1.5 we incorporate vector mesons to the scheme and discuss the problem that arises due to the coupling of the  $\omega$  meson and our solution to it. Finally the last section is devoted to a summary of our main results and to some conclusions we can draw from our study.

## 1.2. Matter at finite density

### 1.2.1. Skyrmion matter

The Skyrme model describes baryons, with arbitrary baryon number, as static soliton solutions of an effective Lagrangian for pions.<sup>2,3</sup> The model has been used to describe not only single baryon properties,<sup>16,30</sup> but also has served to derive the nucleon-nucleon interaction,<sup>3,31</sup> the pion-nucleon interaction,<sup>32</sup> properties of light nuclei and of nuclear matter. In the case of nuclear matter, most of the developments<sup>24,25,33–35</sup> done in late 80's involve a crystal of skyrmions.

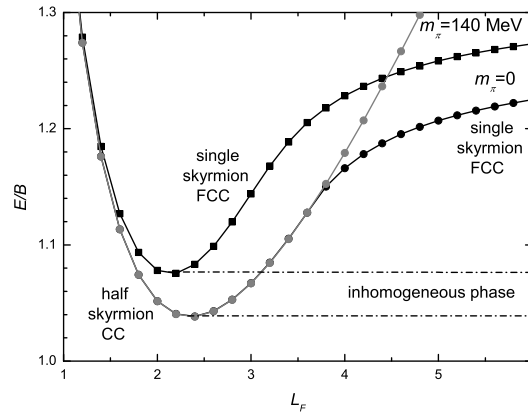


Fig. 1.1. Energy per single skyrmion as a function of the size parameter  $L$ . The solid circles show the results for massless pions and the open circles are those for massive pions. Note the rapid phase transition around  $L \sim 3.8$  for massless pions.

The first attempt to understand the dense skyrmion matter was made by Kutchera *et al.*<sup>36</sup> These authors proceeded by introducing a single skyrmion into a spherical Wigner-Seitz cell without incorporating explicit information on the interaction. The presently considered conventional approaches were developed later. In them one assumes that the skyrmions form a crystal with a specific symmetry and then performs numerical simulations using this symmetry as a constraint. The first guess at this symmetry was made by Klebanov.<sup>24</sup> He considered a system where the skyrmions are located in the lattice site of a cubic crystal (CC) and have relative orientations in such a way that the pair of nearest neighbors attract maximally. Goldhaber and Manton<sup>25</sup> suggested that contrary to Klebanov's findings, the high density phase of skyrmion matter is to be described by a body-centered crystal (BCC) of half skyrmions. This suggestion was confirmed by numerical calculations.<sup>26</sup> Kugler and Shtrikman,<sup>37</sup> using a variational method, investigated the ground state of the skyrmion crystal including not only the single skyrmion CC and half-skyrmion BCC but also the single skyrmion face-centered-cubic crystal (FCC) and half-skyrmion CC. In their calculation a phase transition from the single FCC

to half-skyrmion CC takes place and the ground state is found in the half-skyrmion CC configuration. Castillejo *et al.*<sup>33</sup> obtained similar conclusions.

In Fig. 1.1 we show the energy per baryon  $E/B$  as a function of the FCC box size parameter  $L^a$ . Each point in the figure denotes a minimum of the energy for the classical field configuration associated with the Lagrangians (1.2), (1.4) and (1.6) for a given value of  $L$ . The solid circles correspond to the zero pion mass calculation and reproduce the results of Kugler and Shtrikman.<sup>34</sup> The quantities  $L$  and  $E/B$ , appearing in the figure, are given in units of  $(ef_\pi)^{-1}$  ( $\sim 0.45\text{fm}$  with  $f_\pi = 93\text{ MeV}$  and  $e = 4.75$ ) and  $E/B$  in units of  $(6\pi^2 f_\pi)/e$  ( $\sim 1160\text{ MeV}$ ), respectively. The latter enable us to compare the numerical results on  $E/B$  easily with its Bogolmoln'y bound for the skyrmion in the chiral limit, which can be expressed as  $E/B = 1$  in this convention.

In the chiral limit, as we squeeze the system from  $L = 6$  to around  $L = 3.8$ , one sees that the skyrmion system undergoes a phase transition from the FCC single skyrmion configuration to the CC half-skyrmion configuration. The system reaches a minimum energy configuration at  $L = L_{\min} \sim 2.4$  with the energy per baryon  $E/B \sim 1.038$ . This minimum value is close to the Bogolmoln'y bound for the energy associated to Eqs.(1.2) and (1.4).

On the other hand, the configuration found at  $L > L_{\min}$  with the constrained symmetry may not be the genuine low energy configuration of the system for that given  $L$ . Note that the pressure  $P \equiv \partial E/\partial V$  is negative, which implies that the system in that configuration is unstable. Some of the skyrmions may condense to form dense lumps in the phase leaving large empty spaces forming a stable inhomogeneous as seen in Fig. 1.1 for  $L = L_{\min}$ . Only the phase to the left of the minimum,  $L < L_{\min}$ , may be referred to as “homogeneous” and there the background field is described by a crystal configuration.

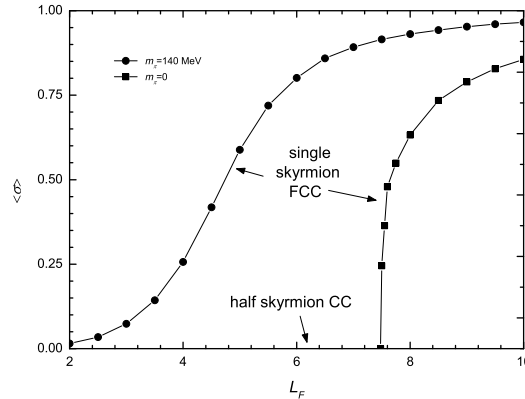


Fig. 1.2.  $\langle \sigma \rangle$  as a function of the size parameter  $L$ . The notation is the same as in Fig. 1.1

<sup>a</sup>A single FCC is a cube with a sidelength  $2L$ , so that there are 4 single skyrmions in a volume of  $8L^3$ , that is, the baryon number density is related to  $L$  as  $\rho_B = 1/2L^3$ .

The open circles are the solutions found with a nonvanishing pion mass,  $m_\pi = 140$  MeV.<sup>b</sup> Comparing to the skyrmion system for massless pions, the energy per baryon is somewhat higher. Furthermore, there is no first order phase transition at low densities.

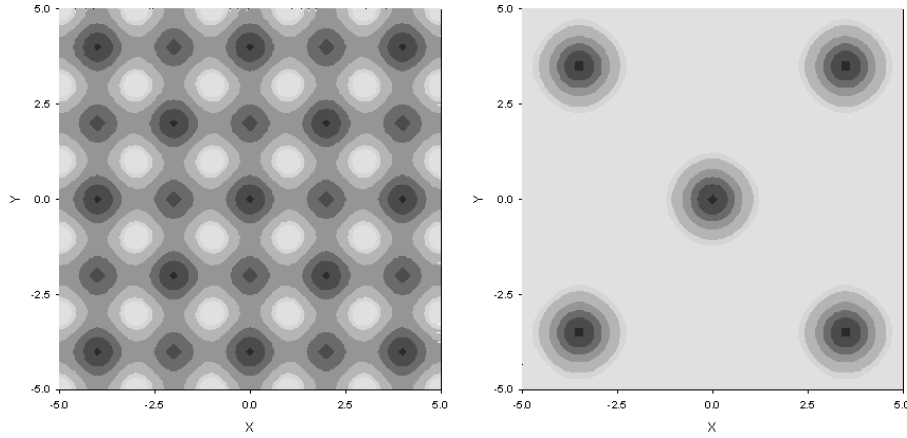


Fig. 1.3. Local baryon number densities at  $L = 3.5$  and  $L = 2.0$  with massive pions. For  $L = 2.0$  the system is (almost) a half-skyrmion in a CC crystal configuration.

In Fig. 1.2, we show  $\langle\sigma\rangle$ , i.e. the space average value of  $\sigma$  as a function of  $L$ . In the chiral limit,  $\langle\sigma\rangle$  rapidly drops as the system shrinks and reaches zero at  $L \sim 3.8$ , where the system goes to the half-skyrmion phase. This phase transition was interpreted<sup>38</sup> as a signal for chiral symmetry restoration. However, as we shall see in the next section, this is not the expected transition. In the case of massive pions, the transition in  $\langle\sigma\rangle$  is soft. Its value decreases monotonically and reaches zero asymptotically, as the density increases. Furthermore, as we can see in Fig. 1.3, where the local baryon number density is shown, for  $L = 2$  (left) and  $L = 3.5$  (right) in the  $z = 0$  plane, the system becomes a half-skyrmion crystal at high density.

Another scheme used to study multi-skyrmion systems is the procedure based on the Atiyah-Manton Ansatz.<sup>39</sup> In this scheme, skyrmions of baryon number  $N$  are obtained by calculating the holonomy of Yang-Mills instantons of charge  $N$ . This Ansatz has been successful in describing few-nucleon systems.<sup>40–42</sup> This procedure has been also applied to nuclear matter with the instanton solution on a four torus.<sup>35</sup> The energy per baryon was found to be  $(E/B)_{min} = 1.058$  at  $L_{min} = 2.47$ , which

<sup>b</sup>Incorporating the pion mass into the problem introduces a new scale in the analysis and therefore we are forced to give specific values to the parameters of the chiral effective Lagrangian, the pion decay constant and the Skyrme parameter, a feature which we have avoided in the chiral limit. In order to proceed, we simply take their empirical values, that is,  $f_\pi = 93$  MeV and  $e = 4.75$ . Although the numerical results depend on these values, their qualitative behavior will not.

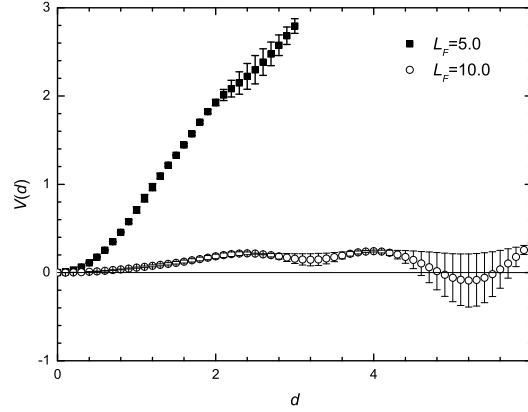


Fig. 1.4. The energy cost to shift a single skyrmion from its stable position by an amount  $d$  in the direction of the  $z$ -axis.

is comparable to the variational result of Kugler and Shtrikman.<sup>37</sup>

In Ref. 43, the Atiyah-Maton Ansatz is employed to get skyrmion matter from the 't Hooft's multi-instanton solution, which is modified to incorporate dynamical variables such as the positions and relative orientations of the single skyrmions. This description provides information on the dynamics of a single skyrmion in skyrmion matter. Shown in Fig. 1.4 is the energy change of the system when a single skyrmion is shifted from its FCC lattice site by an amount  $d$  in the direction of the  $z$ -axis. Two extreme cases are shown. In the case of a dense system ( $L_F \equiv 2L = 5.0$ ), the energy changes abruptly. For small  $d$ , it is almost quadratic in  $d$ . It implies that the dense system is in a crystal phase. On the other hand, in the case of a dilute system ( $L_F = 10.0$ ), the system energy remains almost constant up to some large  $d$ , which implies that the system is in a gas (or liquid) phase. If we let all the variables vary freely, the system will prefer to change to a disordered or inhomogeneous phase in which some skyrmions will form clusters, as we have discussed before.

### 1.2.2. Pions in Skyrmion matter

The Skyrme model also provides the most convenient framework to study the pion properties in dense matter. The basic strategy is to take the static configuration  $U_0(\vec{x})$  discussed in Sec. 1.2.1 as the background fields and to look into the properties of the pion fluctuating on top of it. This is the conventional procedure used to find single particle excitations when one has solitons in a field theory.<sup>44</sup>

The fluctuating *time-dependent* pion fields can be incorporated on top of the static fields through the Ansatz<sup>45</sup>

$$U(\vec{x}, t) = \sqrt{U_\pi} U_0(\vec{x}) \sqrt{U_\pi}, \quad (1.8)$$



where

$$U_\pi = \exp \left( i \vec{\tau} \cdot \vec{\phi}(x) / f_\pi \right), \quad (1.9)$$

with  $\vec{\phi}$  describing the fluctuating pions.

When  $U_0(\vec{r}) = 1$  ( $\rho_B = 0$ ), the expansion in power of  $\phi$ 's leads us to

$$\mathcal{L}(\phi) = \frac{1}{2} \partial_\mu \phi^a \partial^\mu \phi^a + \frac{1}{2} m_\pi^2 \sigma(\vec{x}) \phi^a \phi^a + \dots, \quad (1.10)$$

which is just a Lagrangian for the self-interacting pion fields without any interactions with baryons. Here, we have written only the kinetic and mass terms relevant for further discussions. With a non trivial  $U_0(\vec{r})$  describing dense skyrmion matter, the Lagrangian becomes,

$$\mathcal{L} = \frac{1}{2} G^{ab}(\vec{x}) \partial_\mu \phi_a \partial^\mu \phi_b + \frac{1}{2} m_\pi^2 \sigma(\vec{x}) \phi^a \phi^a + \dots, \quad (1.11)$$

with

$$G^{ab}(\vec{x}) = \sigma^2 \delta_{ab} + \pi_a \pi_b. \quad (1.12)$$

The structure of our Lagrangian is similar to that of chiral perturbation theory Eq. (1.13) of Refs. 46,47. These authors start with a Lagrangian containing all the degrees of freedom, including nucleon fields, and free parameters. They integrate out the nucleons in and out of an à priori assumed Fermi sea and in the process they get a Lagrangian density describing the pion in the medium. Their result corresponds to the above Skyrme Lagrangian except that the quadratic (current algebra) and the mass terms pick up a density dependence of the form

$$- \frac{f_\pi^2}{4} \left( g^{\mu\nu} + \frac{D^{\mu\nu} \rho}{f_\pi^2} \right) \text{Tr}(U^\dagger \partial_\mu U U^\dagger \partial_\nu U) + \frac{f_\pi^2 m_\pi^2}{4} \left( 1 - \frac{\Sigma_{\pi N}}{f_\pi^2 m_\pi^2} \rho \right) \text{Tr}(U + U^\dagger - 2), \quad (1.13)$$

where  $\rho$  is the density of the nuclear matter and  $D^{\mu\nu}$  and  $\sigma$  are physical quantities obtained from the pion-nucleon interactions. Note that in this scheme, nuclear matter is assumed ab initio to be a Fermi sea devoid of the intrinsic dependence mentioned above.

We proceed via a mean field approximation consisting in averaging the background modifications  $G^{ab}(\vec{x})$  and  $\sigma(\vec{x})$  appearing in the Lagrangian which are reduced to constants,  $\langle G^{ab} \rangle = G \delta_{ab}$  and  $\langle \sigma \rangle$ . Then, the Lagrangian can be rewritten as

$$\mathcal{L}(\phi^*) = \frac{1}{2} \partial_\mu \phi_a^* \partial^\mu \phi_a^* + \frac{1}{2} m_\pi^* \phi_a^* \phi_a^* + \dots, \quad (1.14)$$

where we have carried out a wavefunction renormalization,  $\phi_a^* = \sqrt{G} \phi_a$ , which leads to a medium modified pion decay constant and mass as

$$\frac{f_\pi^*}{f_\pi} = \sqrt{G}, \quad (1.15)$$

$$\frac{m_\pi^*}{m_\pi} = \frac{\langle \sigma \rangle}{\sqrt{G}}. \quad (1.16)$$

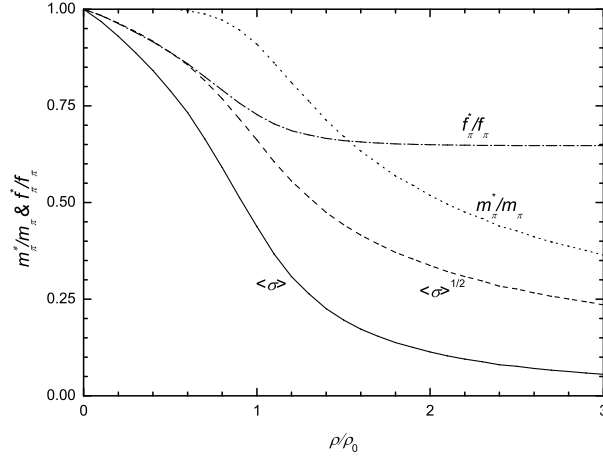


Fig. 1.5. Estimates of  $f_\pi^*/f_\pi$  and  $m_\pi^*/m_\pi$  as functions of the baryon number density of skyrmion matter.

In Fig. 1.5 we show the estimates of  $f_\pi^*/f_\pi$  and  $m_\pi^*/m_\pi$  as a function of the density. As the density increases,  $f_\pi^*$  decreases only to  $\sim 0.65f_\pi$  and then it remains constant at that value. Our result is different from what was the general believe:<sup>38</sup> *the vanishing of  $\langle\sigma\rangle$  is not an indication of chiral symmetry restoration since the pion decay constant does not vanish.*

Note that  $\langle\sigma\rangle^{1/2}$  has the same slope at low densities, which leads to  $m_\pi^*/m_\pi \sim 1$  at low densities. Since at higher densities  $G$  becomes a constant,  $m_\pi^*/m_\pi$  decreases like  $\langle\sigma\rangle^{1/2}$  with a factor which is greater than 1. As the density increases, higher order terms in  $\rho$  come to play important roles and  $m_\pi^*/m_\pi$  decreases. A more rigorous derivation of these quantities can be obtained using perturbation theory.<sup>7</sup>

The slope of  $\langle\sigma\rangle$  at low density is approximately  $1/3$ . If we expand  $\langle\sigma\rangle$  about  $\rho = 0$  and compare it with Eq.(1.13), we obtain

$$\langle\sigma\rangle \sim 1 - \frac{1}{3} \frac{\rho}{\rho_0} + \dots \sim 1 - \frac{\Sigma_{\pi N}}{f_\pi^2 m_\pi^2} \rho + \dots, \quad (1.17)$$

which yields  $\Sigma_{\pi N} \sim m_\pi^2 f_\pi^2 / (3\rho_0) \sim 42$  MeV, which is comparable with the experimental value 45 MeV<sup>c</sup>. This comparison is fully justified from the point of view of the  $\frac{1}{N}$  expansion since both approaches should produce the same result to leading order in this expansion. The liner term is  $\mathcal{O}(1)$ .

The length scale is strongly dependent on our choice of the parameters  $f_\pi$  and  $e$ . Thus one should be aware that the  $\rho$  scale in Fig. 1.5 could change quantitatively considerably if one chooses another parameter set, however the qualitative behavior will remain unchanged.

<sup>c</sup>While this value is widely quoted, there is a considerable controversy on the precise value of this sigma term. In fact it can even be considerably higher than this. See Ref. 48 for a more recent discussion.

Note that the density dependence of the background is taken into account to all orders. No low-density approximation, whose validity is in doubt except at very low density, is ever made in the calculation. The power of our approach is that the dynamics of the background and its excitations can be treated in a unified way on the same footing with a single Lagrangian.

### 1.3. Implementing scale invariance

#### 1.3.1. Dilaton dynamics

The dynamics introduced in Sec. 1.1 as an effective theory for the hadronic interactions is probably incomplete. In fact, it is not clear that the intrinsic density dependence required by the matching to QCD is fully implemented in the model. One puzzling feature is that the Wigner phase represented by the half-skyrmion matter with  $\langle\sigma\rangle = 0$  supports a non-vanishing pion decay constant. This may be interpreted as a possible signal for a pseudogap phase. However, at some point, the chiral symmetry should be restored and there the pion decay constant should vanish.

This difficulty can be circumvented in our framework by incorporating in the standard skyrmion dynamics the trace anomaly of QCD in an effective manner.<sup>20</sup> The end result is the skyrmion Lagrangian introduced by Ellis and Lanik<sup>21</sup> and employed by Brown and Rho<sup>49</sup> for nuclear physics which contains an additional scalar field, the so called scale dilaton.

The classical QCD action of scale dimension 4 in the chiral limit is invariant under the scale transformation

$$x \rightarrow \lambda x = \lambda^{-1}x, \quad \lambda \geq 0, \quad (1.18)$$

under which the quark field and the gluon fields transform with the scale dimension 3/2 and 1, respectively. The quark mass term of scale dimension 3 breaks scale invariance. At the quantum level, scale invariance is also broken by dimensional transmutation even for massless quarks, as signaled by the non-vanishing of the trace of the energy-momentum tensor. Equivalently, this phenomenon can be formulated by the non-vanishing divergence of the dilatation current  $D_\mu$ , the so called trace anomaly,

$$\partial^\mu D_\mu = \theta_\mu^\mu = \sum_q m_q \bar{q}q - \frac{\beta(g)}{g} \text{Tr} G_{\mu\nu} G^{\mu\nu}, \quad (1.19)$$

where  $\beta(g)$  is the beta function of QCD.

Broken scale invariance can be implemented into large  $N_c$  physics by modifying

the standard skyrmion Lagrangian, introduced in Sec. 1.1, to

$$\begin{aligned}\mathcal{L} = & \frac{f_\pi^2}{4} \left( \frac{\chi}{f_\chi} \right)^2 \text{Tr}(\partial_\mu U^\dagger \partial^\mu U) + \frac{1}{32e^2} \text{Tr}([U^\dagger \partial_\mu U, U^\dagger \partial_\nu U])^2 \\ & + \frac{f_\pi^2 m_\pi^2}{4} \left( \frac{\chi}{f_\chi} \right)^3 \text{Tr}(U + U^\dagger - 2) \\ & + \frac{1}{2} \partial_\mu \chi \partial^\mu \chi - \frac{1}{4} \frac{m_\chi^2}{f_\chi^2} \left[ \chi^4 \left( \ln(\chi/f_\chi) - \frac{1}{4} \right) + \frac{1}{4} \right].\end{aligned}\quad (1.20)$$

We have denoted the non vanishing vacuum expectation value of  $\chi$  as  $f_\chi$ , a constant which describes the decay of the scalar into pions. The second term of the trace anomaly (1.19) can be reproduced by the potential energy  $V(\chi)$ , which is adjusted in the Lagrangian (1.20) so that  $V = dV/d\chi = 0$  and  $d^2V/d\chi^2 = m_\chi^2$  at  $\chi = f_\chi$ .<sup>20</sup>

The vacuum state of the Lagrangian at zero baryon number density is defined by  $U = 1$  and  $\chi = f_\chi$ . The fluctuations of the pion and the scalar fields about this vacuum, defined through

$$U = \exp(i\vec{\tau} \cdot \vec{\phi}/f_\pi), \quad \text{and} \quad \chi = f_\chi + \tilde{\chi} \quad (1.21)$$

give physical meaning to the model parameters:  $f_\pi$  as the pion decay constant,  $m_\pi$  as the pion mass,  $f_\chi$  as the scalar decay constant, and  $m_\chi$  as the scalar mass. For the pions, we use their empirical values as  $f_\pi = 93\text{MeV}$  and  $m_\pi = 140\text{MeV}$ . We fix the Skyrme parameter  $e$  to 4.75 from the axial-vector coupling constant  $g_A$  as in Ref. 50. However, for the scalar field  $\chi$ , no experimental values for the corresponding parameters are available.

In Ref. 51, the scalar field is incorporated into a relativistic hadronic model for nuclear matter not only to account for the anomalous scaling behavior but also to provide the mid-range nucleon-nucleon attraction. Then, the parameters  $f_\chi$  and  $m_\chi$  are adjusted so that the model fits finite nuclei. One of the parameter sets is  $m_\chi = 550\text{ MeV}$  and  $f_\chi = 240\text{ MeV}$  (Set A). On the other hand, Song *et al.*<sup>52</sup> obtain the “best” values for the parameters of the effective chiral Lagrangian with the “soft” scalar fields so that the results are consistent with “Brown-Rho” scaling,<sup>49</sup> explicitly,  $m_\chi = 720\text{ MeV}$  and  $f_\chi = 240\text{ MeV}$  (Set B). For completeness, we consider also a parameter set of  $m_\chi = 1\text{ GeV}$  and  $f_\chi = 240\text{ MeV}$  (Set C) corresponding to a mass scale comparable to that of chiral symmetry  $\Lambda_\chi \sim 4\pi f_\pi$ .

### 1.3.2. Dynamics of the single skyrmion

The procedure one has to follow can be found in Ref. 10 and is similar to the one discussed in Sec. 1.2.1. The first step is to find the solution for the single skyrmion which includes the dilaton dynamics. The skyrmion with the baryon number  $B = 1$  can be found by generalizing the spherical hedgehog Ansatz of the original Skyrme model as

$$U_0(\vec{r}) = \exp(i\vec{\tau} \cdot \hat{r}F(r)), \quad \text{and} \quad \chi_0(\vec{r}) = f_\chi C(r), \quad (1.22)$$

with two radial functions  $F(r)$  and  $C(r)$ . Minimization of the mass equation leads to a coupled set of equations of motion for these functions. In order for the solution to carry a baryon number,  $U_0$  has the value  $-1$  at the origin, that is,  $F(x=0) = \pi$ , while there is no such topological constraint for  $C(x=0)$ . All that is required is that it be a positive number below 1. At infinity, the fields  $U_0(\vec{r})$  and  $\chi_0(\vec{r})$  should reach their vacuum values.

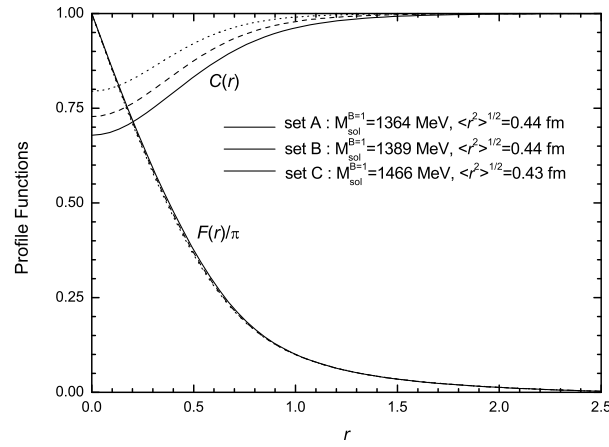


Fig. 1.6. Profile functions  $F(x)$  and  $C(x)$  as a function of  $x$ .

Shown in Fig. 1.6 are profile functions as a function of  $x(=ef_\pi r)$ .  $F(r)$  and consequently the root mean square radius of the baryon charge show little dependence on  $m_\chi$ . On the other hand, the changes in  $C(r)$  and the skyrmion mass are recognizable. Inside the skyrmion, especially at the center,  $C(r)$  deviates from its vacuum value 1. Note that this changes in  $C(r)$  is multiplied by  $f_\pi^2$  in the current algebra term of the Lagrangian. Thus,  $C(r) \leq 1$  reduces the *effective*  $f_\pi$  inside the single skyrmion, which implies a partial restoration of the chiral symmetry there. The reduction in the effective pion decay constant is reflected in the single skyrmion mass.

The larger the scalar mass is, the smaller its coupling to the pionic field and the less its effect on the single skyrmion. In the limit of  $m_\chi \rightarrow \infty$ , the scalar field is completely decoupled from the pions and the model returns back to the original one, where  $C(r) = 1$ ,  $M_{sk} = 1479$  MeV and  $\langle r^2 \rangle^{1/2} = 0.43$  fm.

### 1.3.3. Dense skyrmion matter and chiral symmetry restoration

The second step is to construct a crystal configuration made up of skyrmions with a minimal energy for a given density.

Referring to Refs. 10,11 for the full details, we emphasize here the role the dilaton field in the phase transition scenario for skyrmion matter. Let the dilaton

field  $\chi(\vec{r})$  be a constant throughout the whole space as

$$\chi/f_\chi = X. \quad (1.23)$$

Then the energy per baryon number of the system for a given density can be calculated and conveniently expressed as <sup>10</sup>

$$E/B(X, L) = X^2(E_2/B) + (E_4/B) + X^3(E_m/B) + (2L^3) \left( X^4(\ln X - \frac{1}{4}) + \frac{1}{4} \right), \quad (1.24)$$

where  $E_2$ ,  $E_4$  and  $E_m$  are, respectively, the contributions from the current algebra term, the Skyrme term and the pion mass term of the Lagrangian to the energy of the skyrmion system, described in Sec. 1.1, and  $(2L^3)$  is the volume occupied by a single skyrmion

The quantity  $E/B(X, L)$  can be taken as an *in medium* effective potential for  $X$ , modified by the coupling of the scalar to the background matter. Using the parameter values of Ref. 11 for the Skyrme model without the scalar field, the effective potential  $E/B(X)$  for a few values of  $L$  behaves as shown in Fig. 1.7(a). At low density (large  $L$ ), the minimum of the effective potential is located close to  $X = 1$ . As the density increases, the quadratic term in the effective potential  $E/B(X)$  develops another minimum at  $X = 0$  which is an unstable extremum of the potential  $V(X)$  in free space. At  $L \sim 1$  fm, the newly developed minimum competes with the one near  $X \sim 1$ . At higher density, the minimum shifts to  $X = 0$  where the system stabilizes.

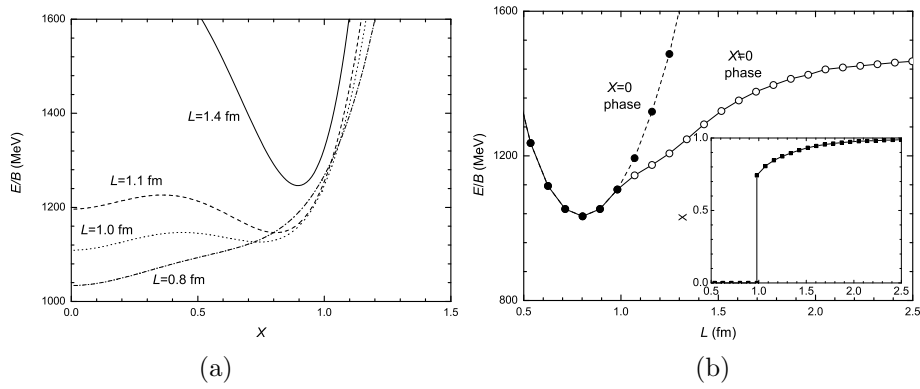


Fig. 1.7. (a) Energy per single skyrmion as a function of the scalar field  $X$  for a given  $L$ . The results are obtained with the  $(E_2/B)$ ,  $(E_4/B)$ , and  $(E_m/B)$  of Ref. 11 and with the parameter sets B, (b) Energy per single skyrmion as a function of  $L$ .

In Fig. 1.7(b), we plot  $E/B(X_{min}, L)$  as a function of  $L$ , which is obtained by minimizing  $E/B(X, L)$  with respect to  $X$  for each  $L$ . The figure in the small box is the corresponding value of  $X_{min}$  as function of  $L$ . There we see the explicit manifestation of a first-order phase transition. Although the present discussion is based on a simplified analysis, it essentially encodes the same physics as in the more

rigorous treatment of  $\chi$  given in Ref. 10

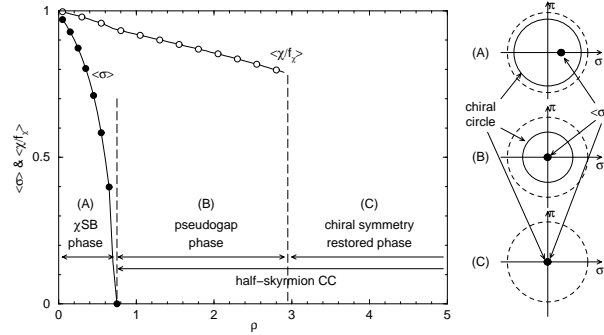


Fig. 1.8. Average values of  $\sigma = \frac{1}{2}\text{Tr}(U)$  and  $\chi/f_\chi$  of the lowest energy crystal configuration at a given baryon number density.

We show in Fig. 1.8 the average values  $\langle\sigma\rangle$  and  $\langle\chi/f_\chi\rangle$  over space for the minimum energy crystal configurations obtained by the complete numerical calculation without any approximation for  $\chi$ . These data show that a ‘structural’ phase transition takes place, characterized by  $\langle\sigma\rangle = 0$ , at lower density than the *genuine* chiral phase transition which occurs when  $\langle\chi\rangle = 0$ . The value of  $\langle\sigma\rangle$  becomes 0 when the structure of the skyrmion crystal undergoes a change from the single skyrmion FCC to the half-skyrmion CC. Thus, the pseudogap phase persists in an intermediate density region, where the  $\langle\chi/f_\chi\rangle$  does not vanish while  $\langle\sigma\rangle$  does.<sup>53</sup> A similar pseudogap structure has been also proposed in hot QCD.<sup>54</sup>

The two step phase transition is schematically illustrated in Fig. 1.8. Let  $\rho_p$  and  $\rho_c$  be the density at which  $\langle\sigma\rangle$  and  $\langle\chi\rangle$  vanish, respectively.

- (A) At low density ( $\rho < \rho_p$ ), matter slightly reduces the vacuum value of the dilaton field from that of the baryon free vacuum. This implies a shrinking of the radius of the chiral circle by the same ratio. Since the skyrmion takes all the values on the chiral circle, the expectation value of  $\sigma$  is not located on the circle but inside the circle. Skyrmion matter at this density is in the chiral symmetry broken phase.
- (B) At some intermediate densities ( $\rho_p < \rho < \rho_c$ ), the expectation value of  $\sigma$  vanishes while that of the dilaton field is still nonzero. The skyrmion crystal is in a CC configuration made of half skyrmions localized at the points where  $\sigma = \pm 1$ . Since the average value of the dilaton field does not vanish, the radius of the chiral circle is still finite. Here,  $\langle\sigma\rangle = 0$  does not mean that chiral symmetry is completely restored. We interpret this as a pseudogap phase.
- (C) At higher density ( $\rho > \rho_c$ ), the phase characterized by  $\langle\chi/f_\chi\rangle = 0$  becomes energetically favorable. Then, the chiral circle, describing the fluctuating pion dynamics, shrinks to a point.

The density range for the occurrence of a pseudogap phase strongly depends on the parameter choice of  $m_\chi$ . For small  $m_\chi$  below 700 MeV, the pseudogap has almost zero size.

In the case of massive pions, the chiral circle is tilted by the explicit (mass) symmetry breaking term. Thus, the exact half-skyrmion CC, which requires a symmetric solution for points with value  $\sigma = +1$  and those with  $\sigma = -1$  cannot be constructed and consequently the phase characterized by  $\langle\sigma\rangle = 0$  does not exist for any density. Thus no pseudogap phase arises. However,  $\langle\sigma\rangle$  is always inside the chiral circle and its value drops much faster than that of  $\langle\chi/f_\chi\rangle$ . Therefore, only if the pion mass is small a pseudogap phase can appear in the model.

#### 1.3.4. Pions in a dense medium with dilaton dynamics

Since we have achieved, via dilaton dynamics, a reasonable scenario for chiral symmetry restoration, it is time to revisit the properties of pions in a dense medium. As was explained in Sec. 1.2.2 and in Ref. 7, we proceed to incorporate the fluctuations on top of the static skyrmion crystal. (We refer to Refs. 10,11 for details.)

Using a mean field approximation we calculate the in-medium pion mass  $m_\pi^*$  and decay constant  $f_\pi^*$  obtaining,

$$Z_\pi^2 = \left\langle \left( \frac{\chi_0(\vec{x})}{f_\chi} \right)^2 \left( 1 - \frac{2}{3} \pi^2(\vec{x}) \right) \right\rangle \equiv \left( \frac{f_\pi^*}{f_\pi} \right)^2, \quad (1.25)$$

$$m_\pi^{*2} Z_\pi^2 = \left\langle \left( \frac{\chi_0(\vec{x})}{f_\chi} \right)^3 \sigma(\vec{x}) m_\pi^2 \right\rangle. \quad (1.26)$$

The wave function renormalization constant  $Z_\pi$  gives the ratio of the in-medium pion decay constant  $f_\pi^*$  to the free one, and the above expression arises from the current algebra term in the Lagrangian. The explicit calculation of  $m_\chi^*$  is given in Ref. 11.

In Fig. 1.9 we show the (exact) ratios of the in-medium parameters relative to their free-space values. Only the results obtained with the parameter set B are shown. The parameter set A yields similar results while set C shows a two step structure with an intermediate pseudogap phase. Not only the average value of  $\chi_0$  over the space but also  $\chi_0(\vec{r})$  itself vanishes at any point in space. This is the reason for the vanishing of  $m_\pi^*$  and  $f_\pi^*$ . That is,  $f_\pi^*$  really vanishes when  $\rho < \rho_c$  in the Skyrme model with dilaton dynamics.

At low matter density, the ratio  $f_\pi^*/f_\pi$  can be fitted to a linear function

$$\frac{f_\pi^*}{f_\pi} \sim 1 - 0.24(\rho/\rho_0) + \dots \quad (1.27)$$

At  $\rho = \rho_0$ , this yields  $f_\pi^*/f_\pi = 0.76$ , which is comparable to the other predictions.

In Ref. 11, the in medium modification of the  $\chi$  decay into two pions is also studied using the mean field approximation. Gathering the terms with a fluctuating



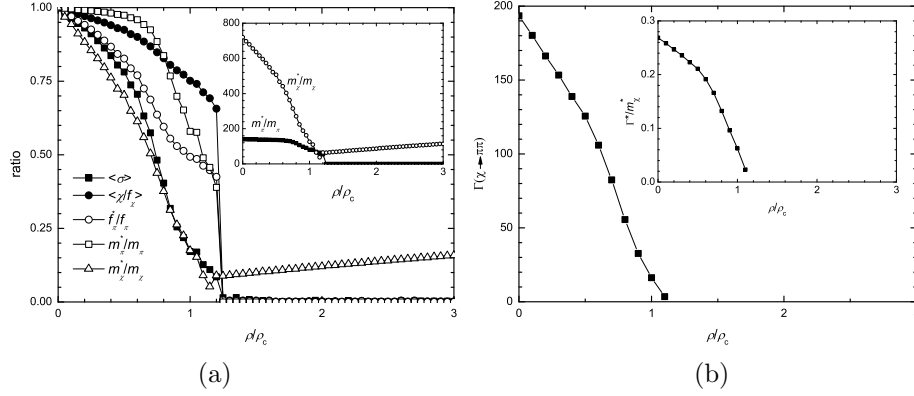


Fig. 1.9. (a) The ratios of the in-medium parameters to the free space parameters. The graph in a small box shows the masses of the pion and the scalar, (b) the in-medium decay width  $\Gamma^*(\chi \rightarrow \pi\pi)$  as a function of  $\rho$ .

scalar field and two fluctuating pion fields, we get the Lagrangian density for the process  $\chi \rightarrow \pi\pi$

$$\mathcal{L}_{M,\chi\pi^2} = \frac{\chi_0}{f_\chi^2} (\delta_{ab} + g_{ab}) \chi \partial_\mu \phi_a \partial^\mu \phi_b, \quad (1.28)$$

where only the term from  $\mathcal{L}_\sigma$  is used. Averaging the space dependence of the background field configuration modifies the coupling constant by a factor  $\langle (\chi_0/f_\chi)(1 + g_{11}) \rangle = \langle (\chi_0/f_\chi)(1 - \frac{2}{3}\pi^2) \rangle$ . Taking into account the appropriate wave function renormalization factors,  $Z_\pi$ , and the change in the scalar mass, we obtain the in-medium decay width as

$$\Gamma^*(\chi \rightarrow \pi\pi) = \frac{3m_\chi^{*3}}{32\pi f_\chi^2} \left| \frac{\langle (\chi_0/f_\chi)(1 - \frac{2}{3}\pi^2) \rangle}{\langle (\chi_0/f_\chi)^2(1 - \frac{2}{3}\pi^2) \rangle} \right|^2 \approx \frac{3m_\chi^{*3}}{32\pi f_\chi^{*2}}. \quad (1.29)$$

We show in Fig. 1.9 the in-medium decay width predicted with the parameter set B. In the region  $\rho \geq \rho_{pt}$  where  $\chi_0 = 0$ ,  $\Gamma^*$  cannot be defined to this order. Near the critical point, the scalar becomes an extremely narrow-width excitation, a feature which has been discussed in the literature as a signal for chiral restoration.<sup>55,56</sup>

Another interesting change in the properties of the pion in the medium is associated with the in medium pion dispersion relation. This relation requires, besides the mass, the so-called in medium pion velocity,  $v_\pi$ . This property allows us to gain more insight into the real time properties of the system under extreme conditions and enables us to analyze how the phase transition from normal matter to deconfined QCD takes place from the hadronic side, the so called ‘bottom up’ approach.

At nonzero temperature and/or density, the Lorentz symmetry is broken by the medium. In the dispersion relation for the pion modes (in the chiral limit)

$$p_0^2 = v_\pi^2 |\vec{p}|^2, \quad (1.30)$$

the velocity  $v_\pi$  which is 1 in free-space must depart from 1. This may be studied reliably, at least at low temperatures and at low densities, via chiral perturbation theory.<sup>57</sup> The in-medium pion velocity can be expressed in terms of the time component of the pion decay constant,  $f_\pi^t$  and the space component,  $f_\pi^s$ ,<sup>58,59</sup>

$$\begin{aligned}\langle 0|A_a^0|\pi^b(p)\rangle_{\text{in-medium}} &= i f_\pi^t \delta^{ab} p^0, \\ \langle 0|A_a^i|\pi^b(p)\rangle_{\text{in-medium}} &= i f_\pi^s \delta^{ab} p^i.\end{aligned}\quad (1.31)$$

The conservation of the axial vector current leads to the dispersion relation (1.30) with the pion velocity given by

$$v_\pi^2 = f_\pi^s / f_\pi^t. \quad (1.32)$$

In Ref. 60 two decay constants,  $f_t$  and  $f_s$ , are defined differently from those of Eq.(1.31), through the effective Lagrangian,

$$\mathcal{L}_{\text{eff}} = \frac{f_t^2}{4} \text{Tr}(\partial_0 U^\dagger \partial_0 U) - \frac{f_s^2}{4} \text{Tr}(\partial_i U^\dagger \partial_i U) + \dots, \quad (1.33)$$

where  $U$  is an SU(2)-valued chiral field whose phase describes the in-medium pion. In terms of these constants, the pion velocity is defined by

$$v_\pi = f_s / f_t. \quad (1.34)$$

In Ref. 11, it is shown that local interactions with background skyrmion matter lead to a breakdown of Lorentz symmetry in the dense medium and to an effective Lagrangian for pion dynamics in the form of Eq.(1.33). The results are shown in Figs. 1.10. Both of the pion decay constants change significantly as a function of density and vanish – in the chiral limit – when chiral symmetry is restored. However, the second-order contributions to the  $f_s$  and  $f_\pi$ , which break Lorentz symmetry, turn out to be rather small, and thus their ratio, the pion velocity, stays  $v_\pi \sim 1$ . The lowest value found is  $\sim 0.9$ . Note, however, the drastic change in its behavior at two different densities. At the lower density, where skyrmion matter is in the chiral symmetry broken phase, the pion velocity decreases and has the minimum at  $\rho = \rho_p$ . If one worked only at low density in a perturbative scheme, one would conclude that the pion velocity decreases all the way to zero. However, the presence of the pseudogap phase transition changes this behavior. In the pseudogap phase, the pion velocity not only stops decreasing but starts increasing with increasing density. In the chiral symmetry restored phase both  $f_t$  and  $f_s$  vanish. Thus their ratio makes no sense.

In Refs. 12,13, the in-medium modification of the neutral pion decay process into two gammas and neutrino-anti-neutrino pair are studied in the same manner. The  $\pi^0 \rightarrow \gamma\gamma$  process is shown to be strongly suppressed in dense medium, while the process  $\pi^0 \rightarrow \nu\bar{\nu}$  forbidden in free space becomes possible by the Lorentz symmetry breaking effect of the medium.

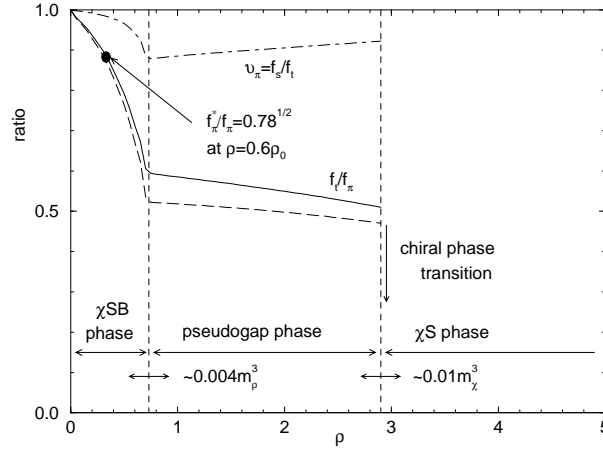


Fig. 1.10. In-medium pion decay constants and their ratio, the pion velocity.

#### 1.4. Skyrmion matter at finite temperature

There are many studies of lattice QCD at finite temperature. The situation is completely different for skyrmion matter where the number of studies is limited. For example, skyrmion matter has been heated up to melt the crystal into a liquid to study the crystal-liquid phase transition.<sup>28,29</sup> However this phenomenon is irrelevant to study the restoration of chiral symmetry, which interests us here for the reasons discussed in previous sections.

What happens if we heat up the system? Naively, as the temperature increases, the kinetic energy of the skyrmions increases and the skyrmion crystal begins to melt. The kinetic energy associated with the translations, vibrations and rotations of the skyrmions is proportional to  $T$ . This mechanism leads to a solid-liquid-gas phase transition of the skyrmion system. However, we are interested in the chiral symmetry restoration transition, which is not related to the melting. Therefore, a new mechanism must be incorporated to describe chiral symmetry restoration. We show in what follows that the thermal excitation of the pions in the medium is the appropriate mechanism, since this phenomenon is proportional to  $T^4$  and therefore dominates the absorption of heat.

The pressure of non-interacting pions is given by <sup>61</sup>

$$P = \frac{\pi^2}{30} T^4, \quad (1.35)$$

where we have taken into account the contributions from three species of pion,  $\pi^+, \pi^0, \pi^-$ . This term contributes to the energy per single skyrmion volume as  $3PV(\chi/f_\chi)^2$ . The kinetic energy of the pions arises from  $\mathcal{L}_\sigma$  (1.2), and therefore scale symmetry implies that it should carry a factor  $\chi^2$ . The factor 3 comes from the fact that our pions are massless.

To estimate the properties of skyrmion matter at finite temperature let us take  $\chi$  as a constant field as we did in Sec. 1.3.3. After including thermal pions, Eq. (1.24) can be rewritten as

$$E/B(\rho, T, X) = \left( E_2/B(\rho) + \frac{\pi^2}{10} T^4 V \right) X^2 + (E_4/B(\rho) + X^4 (\ln X - \frac{1}{4}) + \frac{1}{4}), \quad (1.36)$$

where we have dropped the pion mass term.

As in Sec. 1.3.3, chiral restoration will occur when the value of  $X_{\min}$  that minimizes  $E/B$  vanishes. By minimizing  $E/B$  with respect to  $X$ , we observe that the phase transition from a non-vanishing  $X = e^{-1/4}$  to  $X = 0$ . Thus, the nature of the phase transition is of the first order.

After a straightforward calculation we obtain,

$$\rho^c(E_2/B) + \frac{\pi^2}{10} T_c^4 = \frac{f_\chi^2 m_\chi^2}{8e^{1/2}}. \quad (1.37)$$

which leads to

$$T_c = \left( \frac{10}{\pi^2} \left( \frac{f_\chi^2 m_\chi^2}{8e^{1/2}} - \rho^c(E_2/B)(\rho^c) \right) \right)^{1/4} \quad (1.38)$$

For  $\rho = 0$  (zero density), our estimate for the critical temperature is

$$T_c = \left( \frac{10}{\pi^2} \frac{f_\chi^2 m_\chi^2}{8e^{1/2}} \right)^{1/4} \sim 205 \text{ MeV}, \quad (1.39)$$

where we have used the following values for the parameters.  $f_\chi = 210$  MeV and  $m_\chi = 720$  MeV. It is remarkable that our model leads to  $T_c \sim 200$  MeV, which is close to that obtained by lattice QCD<sup>4</sup> and in agreement with the data.<sup>62</sup> To us this is a confirmation that the mechanism chosen for the absorption of heat plays a fundamental role in the hadronic phase.

The numerical results on  $E_2/B$  that minimize the energy of the system for a given  $\rho_B$  can be approximated by

$$E_2/B = \begin{cases} 10f_\pi^2/\rho^{1/3}, & \rho > \rho_0 \\ 36f_\pi/e_{\text{sk}}, & \rho < \rho_0, \end{cases} \quad (1.40)$$

where  $\rho_0 = (e_{\text{sk}} f_\pi / 3.6)^3$ .

Using Eq.(1.40) for  $E_2/B$ , we obtain the critical density for chiral symmetry restoration at zero temperature as

$$\rho^c(T=0) = \left( \frac{f_\chi^2 m_\chi^2}{8e^{1/2}} \frac{1}{10f_\pi^2} \right)^{3/2} \sim 0.37 \text{ fm}^{-3}. \quad (1.41)$$

Since  $\rho_0 = 0.24 \text{ fm}^{-3} < \rho^c(T=0)$  our result is consistent with the high density formula for  $E_2/B$  used.

The resulting critical density  $\rho^c(T=0) \sim 0.37 \text{ fm}^{-3}$  is only twice normal nuclear matter density and it is low with respect to the expected values. This result does

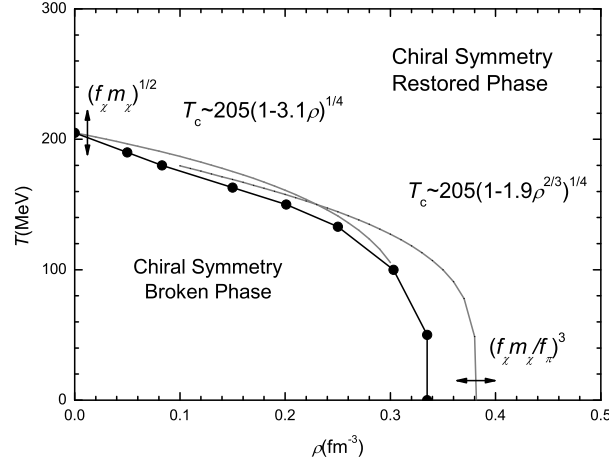


Fig. 1.11. The chiral phase transition. The solid line shows the exact calculation, while the gray lines two approximate estimates.

not represent a problem since  $\rho^c(T=0)$  scales with  $(f_\chi m_\chi / f_\pi)^3$  and  $T_c^{\rho=0}$  with  $(f_\chi m_\chi)^{1/2}$  and small changes in the parameters lead to larger values for the critical density without changing the critical temperature too much.

For a finite density smaller than  $\rho^c(T=0)$ , we obtain the corresponding critical temperature by substituting the asymptotic formulas (1.40) for  $E_2/B$ ,

$$T_c = \begin{cases} T_c(\rho=0) (1 - 3.09 \rho_c)^{1/4} & \text{for } \rho < \rho_0, \\ T_c(\rho=0) (1 - 1.92 \rho_c^{2/3})^{1/4} & \text{for } \rho > \rho_0, \end{cases} \quad (1.42)$$

where the density is measured in  $\text{fm}^{-3}$ . The gray lines in Fig. 1.11 show these two curves. The results from the *exact* calculations obtained by minimization of the energy (1.36) are shown by black dots connected by black line in Fig. 1.11. The resulting phase diagram has the same shape but the values of the temperatures and densities are generally smaller than in the approximate estimates.

### 1.5. Vector mesons and dense matter

In our effort to approach the theory of the hadronic interactions and inspired by Weinberg's theorem<sup>19</sup> we proceed to incorporate to the model the lowest-lying vector mesons, namely the  $\rho$  and the  $\omega$ . In this way we also do away with the ad hoc Skyrme quartic term. It is known that these vector mesons play a crucial role in stabilizing the single nucleon system<sup>30,63</sup> as well as in the saturation of normal nuclear matter.<sup>64</sup>

We consider a skyrmion-type Lagrangian with vector mesons possessing hidden local gauge symmetry,<sup>22</sup> spontaneously broken chiral symmetry and scale symmetry.<sup>10,21</sup> Such a theory might be considered as a better approximation to reality

than the extreme large  $N_c$  approximation to QCD represented by the Skyrme model. Specifically, the model Lagrangian, which we investigate, is given by <sup>65</sup>

$$\begin{aligned} \mathcal{L} = & \frac{f_\pi^2}{4} \left( \frac{\chi}{f_\chi} \right)^2 \text{Tr}(\partial_\mu U^\dagger \partial^\mu U) + \frac{f_\pi^2 m_\pi^2}{4} \left( \frac{\chi}{f_\chi} \right)^3 \text{Tr}(U + U^\dagger - 2) \\ & - \frac{f_\pi^2}{4} a \left( \frac{\chi}{f_\chi} \right)^2 \text{Tr}[\ell_\mu + r_\mu + i(g/2)(\vec{\tau} \cdot \vec{\rho}_\mu + \omega_\mu)]^2 - \frac{1}{4} \vec{\rho}_{\mu\nu} \cdot \vec{\rho}^{\mu\nu} - \frac{1}{4} \omega_{\mu\nu} \omega^{\mu\nu} \\ & + \frac{3}{2} g \omega_\mu B^\mu + \frac{1}{2} \partial_\mu \chi \partial^\mu \chi - \frac{m_\chi^2 f_\chi^2}{4} [(\chi/f_\chi)^4 (\ln(\chi/f_\chi) - \frac{1}{4}) + \frac{1}{4}], \end{aligned} \quad (1.43)$$

where,  $U = \exp(i\vec{\tau} \cdot \vec{\pi}/f_\pi) \equiv \xi^2$ ,  $\ell_\mu = \xi^\dagger \partial_\mu \xi$ ,  $r_\mu = \xi \partial_\mu \xi^\dagger$ ,  $\vec{\rho}_{\mu\nu} = \partial_\mu \vec{\rho}_\nu - \partial_\nu \vec{\rho}_\mu + g \vec{\rho}_\mu \times \vec{\rho}_\nu$ ,  $\omega_{\mu\nu} = \partial_\mu \omega_\nu - \partial_\nu \omega_\mu$ , and  $B^\mu = \frac{1}{24\pi^2} \epsilon^{\mu\nu\alpha\beta} \text{Tr}(U^\dagger \partial_\nu U U^\dagger \partial_\alpha U U^\dagger \partial_\beta U)$ . Note that the Skyrme quartic term is not present. The vector mesons,  $\rho$  and  $\omega$ , are incorporated as dynamical gauge bosons for the local hidden gauge symmetry of the non-linear sigma model Lagrangian and the dilaton field  $\chi$  is introduced so that the Lagrangian has the same scaling behavior as QCD. The physical parameters appearing in the Lagrangian are summarized in Table 1.1.

Table 1.1. Parameters of the model Lagrangian

| notation | physical meaning               | value                |
|----------|--------------------------------|----------------------|
| $f_\pi$  | pion decay constant            | 93 MeV               |
| $f_\chi$ | $\chi$ decay constant          | 210 MeV              |
| $g$      | $\rho\pi\pi$ coupling constant | 5.85*                |
| $m_\pi$  | pion mass                      | 140 MeV              |
| $m_\chi$ | $\chi$ mass                    | 720 MeV              |
| $m_V$    | vector meson masses            | 770 MeV <sup>†</sup> |
| $a$      | vector meson dominance         | 2                    |

\* obtained by using the KSFR relation  $m_V^2 = m_\rho^2 = m_\omega^2 = a f_\pi^2 g^2$  with  $a = 2$ . cf.  $g_{\rho\pi\pi} = 6.11$  from the decay width of  $\rho \rightarrow \pi\pi$ .

<sup>†</sup> experimentally measured values are  $m_\rho = 768$  MeV and  $m_\omega = 782$  MeV.

### 1.5.1. Dynamics of the single skyrmion

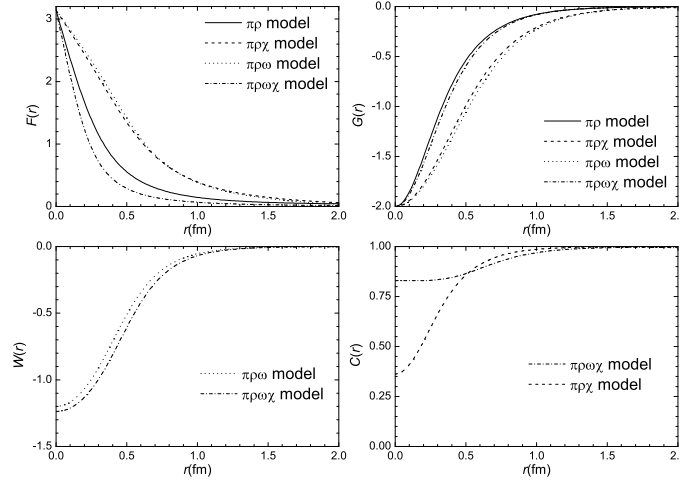
The spherically symmetric hedgehog Ansatz for the  $B = 1$  soliton solution of the standard Skyrme model can be generalized to

$$U^{B=1} = \exp(i\vec{\tau} \cdot \hat{r} F(r)), \quad (1.44)$$

$$\rho_{\mu=i}^{a,B=1} = \varepsilon^{ika} \hat{r}^k \frac{G(r)}{gr}, \quad \rho_{\mu=0}^{a,B=1} = 0, \quad (1.45)$$

$$\omega_{\mu=i}^{B=1} = 0, \quad \omega_{\mu=0}^{B=1} = f_\pi W(r), \quad (1.46)$$

$$\chi^{B=1} = f_\chi C(r). \quad (1.47)$$

Fig. 1.12. Profile functions -  $F(r)$ ,  $G(r)$ ,  $W(r)$  and  $C(r)$ .

The boundary conditions that the profile functions satisfy at infinity are

$$F(\infty) = G(\infty) = W(\infty) = 0, \quad C(\infty) = 1, \quad (1.48)$$

and at the center ( $r = 0$ ) are

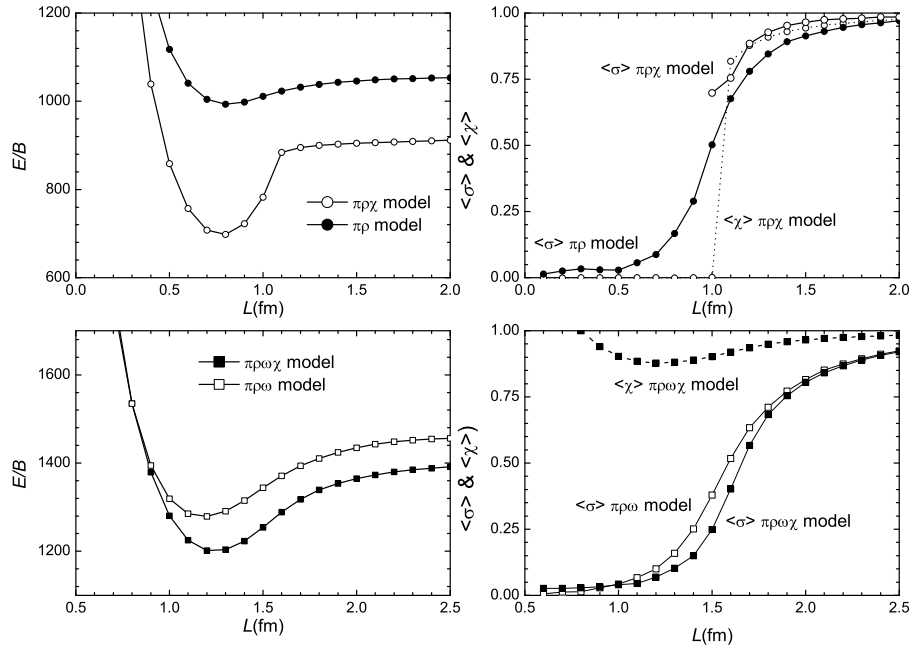
$$F(0) = \pi, \quad G(0) = -2, \quad W'(0) = C'(0) = 0. \quad (1.49)$$

The profile functions are obtained numerically by minimizing the soliton mass with the boundary conditions (see Ref. 8 for the technical details). The results are summarized in Table 1.2 and the corresponding profile functions are given in Fig. 1.12. The role of the  $\omega$  meson that provides a strong repulsion is prominent. Comparing the  $\pi\rho$  model with the  $\pi\rho\omega$  model, the presence of the  $\omega$  increases the mass by more than 415 MeV and the size, i.e.  $\langle r^2 \rangle$ , by more than .28 fm<sup>2</sup>.

How does the dilaton affect this calculation? The  $\pi\rho$  model with much smaller skyrmion has a larger baryon density near the origin and this affects the dilaton, significantly changing its mean-field value from its vacuum one. The net effect of the dilaton mean field on the mass is a reduction of  $\sim 150$  MeV, whereas for the  $\pi\rho\omega$  model it is only of 50 MeV. The details can be seen in Table 1.2. The effect on the soliton size is, however, different: while the dilaton in the  $\pi\rho$  model produces an additional localization of the baryon charge and hence reduces  $\langle r^2 \rangle$  from .21 fm<sup>2</sup> to .19 fm<sup>2</sup>, in the  $\pi\rho\omega$  model, on the contrary, the dilaton produces a *delocalization* and increases  $\langle r^2 \rangle$  from .49 fm<sup>2</sup> to .51 fm<sup>2</sup>. We will see, however, that this strong repulsion provided by  $\omega$  causes a somewhat serious problem in the chiral restoration of the skyrmion matter at higher density.

Table 1.2. Single skyrmion mass and various contributions to it.

| Model                      | $\langle r^2 \rangle$ | $E^{B=1}$ | $E_{\pi}^{B=1}$ | $E_{\pi\rho}^{B=1}$ | $E_{\rho}^{B=1}$ | $E_{\omega}^{B=1}$ | $E_{WZ}^{B=1}$ | $E_{\chi}^{B=1}$ |
|----------------------------|-----------------------|-----------|-----------------|---------------------|------------------|--------------------|----------------|------------------|
| $\pi\rho$ -model           | 0.27                  | 1054.6    | $400.2 + 9.2$   | 110.4               | 534.9            | 0.0                | 0.0            | 0.0              |
| $\pi\rho\chi$ -model       | 0.19                  | 906.5     | $103.1 + 1.4$   | 155.1               | 504.1            | 0.0                | 0.0            | 142.8            |
| $\pi\rho\omega$ -model     | 0.49                  | 1469.0    | $767.6 + 39.9$  | 33.2                | 370.7            | -257.6             | 515.1          | 0.0              |
| $\pi\rho\omega\chi$ -model | 0.51                  | 1408.3    | $646.0 + 29.2$  | 34.9                | 355.7            | -278.3             | 556.7          | 64.2             |

Fig. 1.13.  $E/B$ ,  $\langle\chi\rangle$  and  $\langle\sigma\rangle$  as a function of  $L$  in the models (a) without the  $\omega$  and (b) with  $\omega$ .

### 1.5.2. Skyrmion Matter : an FCC skyrmion crystal

Again, the lowest-energy configuration is obtained when one of the skyrmions is rotated in isospin space with respect to the other by an angle  $\pi$  about an axis perpendicular to the line joining the two.<sup>8</sup> If we generalize this Ansatz to many-skyrmion matter, we obtain that the configuration at the classical level for a given baryon number density is an FCC crystal where the nearest neighbour skyrmions are arranged to have the attractive relative orientations.<sup>7</sup> Kugler's Fourier series expansion method<sup>37</sup> can be generalized to incorporate the vector mesons, although some subtleties associated with the vector fields have to be implemented. The details can be found in Ref. 8.

Figs. 1.13 are the numerical results of the energy per baryon  $E/B$ ,  $\langle\chi\rangle$  and  $\langle\sigma\rangle$  in various models as a function of the FCC lattice parameter  $L$ . In the  $\pi\rho\chi$



model, as the density of the system increases ( $L$  decreases),  $E/B$  changes little. It is close to the energy of a  $B = 1$  skyrmion up to a density greater than  $\rho_0$  ( $L \sim 1.43$ ). This result is easy to interpret. As we discussed before the size of the skyrmion in this model is very small and therefore the skyrmions in the lattice will interact only at very high densities, high enough for their tails to overlap.

In the absence of the  $\omega$ , the dilaton field plays a dramatic role. A skyrmion matter undergoes an abrupt phase transition at high density at which the expectation value of the dilaton field vanishes  $\langle\chi\rangle = 0$ . (In general,  $\langle\chi\rangle = 0$  does not necessarily require  $\langle\chi^2\rangle = 0$ . However, since  $\chi \geq 0$ ,  $\langle\chi\rangle = 0$  always accompanies  $\chi = 0$  in the whole space.) The  $\rho$  meson on the other hand is basically a spectator at the classical level, producing little change with respect to our previously studied  $\pi\chi$  model except that at high densities, once the  $\rho$  starts to overlap, the energy of nuclear matter increases due to its repulsive effect at short distances. The densities have to be quite high since these skyrmions are very small. Since  $\chi$  vanishes at the phase transition, we recover the standard behavior, namely,  $f_\pi^* = 0$  and  $m_\rho^* = 0$ .

In the  $\pi\rho\omega\chi$  model, the situation changes dramatically. The reason is that the  $\omega$  provides not only a strong repulsion among the skyrmions, but somewhat surprisingly, also an intermediate range attraction. Note the different mass scales between Figs. 1.13(a) and 1.13(b). In both the  $\pi\rho\omega$  and the  $\pi\rho\omega\chi$  models, at high density, the interaction reduces  $E/B$  to 85% of the  $B = 1$  skyrmion mass. This value should be compared with 94% in the  $\pi\rho$  model. In the  $\pi\rho\chi$ -model,  $E/B$  goes down to 74% of the  $B = 1$  skyrmion mass, but in this case it is due to the dramatic behavior of the dilaton field.

In the  $\pi\rho\omega\chi$  model the role of the dilaton field is suppressed. It provides a only a small attraction at intermediate densities. Moreover, the phase transition towards its vanishing expectation value,  $\langle\chi\rangle = 0$ , does not take place. Instead, its value grows at high density!

The problem involved is associated with the Lagrangian (1.43) which includes an anomalous part known as Wess-Zumino term, namely the coupling of the  $\omega$  to the Baryon current,  $B_\mu$ . To see that this term is the one causing the problem, consider the energy per baryon contributed by this term.<sup>8</sup>

$$\left(\frac{E}{B}\right)_{WZ} = \frac{1}{4} \left(\frac{3g}{2}\right)^2 \int_{Box} d^3x \int d^3x' B_0(\vec{x}) \frac{\exp(-m_\omega^*|\vec{x} - \vec{x}'|)}{4\pi|\vec{x} - \vec{x}'|} B_0(\vec{x}') \quad (1.50)$$

where “Box” corresponds to a single FCC cell. Note that while the integral over  $\vec{x}$  is defined in a single FCC cell, that over  $\vec{x}'$  is not. Thus, unless it is screened, the periodic source  $B_0$  filling infinite space will produce an infinite potential  $w$  which leads to an infinite  $(E/B)_{WZ}$ . The screening is done by the omega mass,  $m_\omega^*$ . Thus the effective  $\omega$  mass cannot vanish. Our numerical results reflect this fact: at high density the  $B_0$ - $B_0$  interaction becomes large compared to any other contribution. In order to reduce it,  $\chi$  has to increase, and thereby the effective screening mass  $m_\omega^* \sim m_\omega \langle\chi\rangle$  becomes larger. In this way we run into a phase transition where the expectation value of  $\chi$  does not vanish and therefore  $f_\pi$  does not vanish but instead

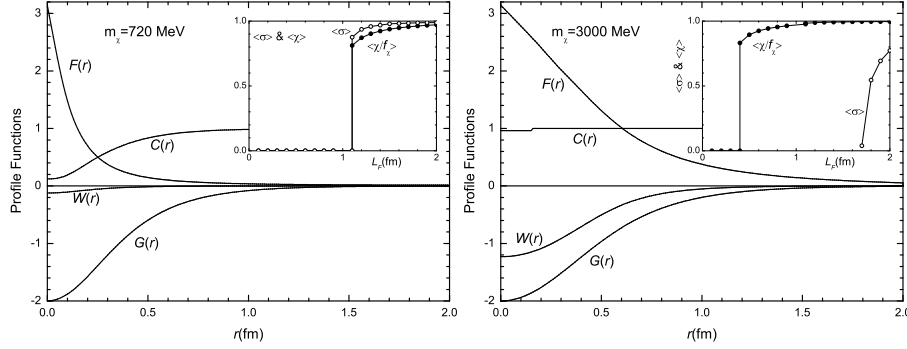


Fig. 1.14. A small and large skyrmion obtained with  $m_\chi = 720$  MeV (left) and  $m_\chi = 3000$  MeV. Shown in small boxes are  $\langle\chi\rangle$  and  $\langle\sigma\rangle$  as a function of the FCC lattice size  $L_F$ .

increases.

### 1.5.3. A Resolution of the $\omega$ problem

Assuming that there is nothing wrong with (1.43), we focus on the Wess-Zumino term in the Lagrangian. Our objective is to find an alternative to (1.43) that leads to a behavior consistent with the expected behavior. In the absence of any reliable clue, we try the simplest, admittedly *ad hoc*, modification of the Lagrangian (1.43) that allows a reasonable and appealing way-out.<sup>9</sup> Given our ignorance as to how spontaneously broken scale invariance manifests in matter, we shall simply forego the requirement that the anomalous term be scale invariant and multiply the anomalous  $\omega \cdot B$  term by  $(\chi/f_\chi)^n$  for  $n \geq 2$ . We have verified that it matters little whether we pick  $n = 2$  or  $n = 3$ .<sup>9</sup> We therefore take  $n = 3$ :

$$L'_{an} = \frac{3}{2}g(\chi/f_\chi)^3\omega_\mu B^\mu \quad (1.51)$$

This additional factor has two virtues:

- i) It leaves meson dynamics in free space (i.e.  $\chi/f_\chi = 1$ ) unaffected, since chiral symmetry is realized à la sigma model as required by QCD.
- ii) It plays the role of an effective density-dependent coupling constant so that at high density, when scale symmetry is restored and  $\chi/f_\chi \rightarrow 0$ , there will be no coupling between the  $\omega$  and the baryon density as required by hidden local symmetry with the vector manifestation.

The properties of this Lagrangian for the meson ( $B = 0$ ) sector are the same as in our old description. The parameters of the Lagrangian are determined by meson physics as given in Table 1.1

Fig. 1.14 summarizes the consequences of the modification. Depending on the dilaton mass, the properties of a single skyrmion show distinguished characters

and consequently undergoes different phase transition. A small dilaton mass, say  $m_\chi \sim 1$  GeV, leads to a very small skyrmion with an rms radius about 0.1 fm. The light dilaton seems to react quite sensitively to the presence of the matter. One can see that at the center of the single skyrmion the chiral symmetry is almost restored. It weakens most of the repulsion from  $\omega - B$  coupling, which leads us to such a small sized skyrmion. Since these small skyrmions are already chiral-symmetry-restored objects, simply filling the space with them restores the symmetry. As shown in the small box, chiral symmetry is restored simultaneously when  $\langle \sigma \rangle$  vanishes. In case of having a large mass, the dilaton does not play any significant role in the structure of a single skyrmion. This scenario leads, as the density of skyrmion matter increases, first to a pseudogap phase transition where  $\langle \sigma \rangle = 0$  and thereafter, at higher density, to a genuine chiral symmetry restoration phase transition where  $\langle \chi/f_\chi \rangle = 0$ . Anyway, whether the dilaton is light or heavy, we finally have a reasonable phase transition scenario that at some critical density chiral symmetry restoration occurs where  $\langle \chi/f_\chi \rangle$  vanishes.

Under the same mean field approximation, this skyrmion approach to the dense matter leads us to the scaling behaviors of the vector mesons

$$\frac{m_\rho^*}{m_\rho} = \frac{m_\omega^*}{m_\omega} = \sqrt{\left\langle \left( \frac{\chi}{f_\chi} \right)^2 \right\rangle}, \quad (1.52)$$

while that of the pion decay constant is

$$\frac{f_\pi^*}{f_\pi} = \sqrt{\left\langle \left( \frac{\chi}{f_\chi} \right)^2 \left( 1 + (a-1) \frac{2}{3} \pi^2 \right) \right\rangle}. \quad (1.53)$$

With  $a = 1$ , a remarkably simple BR scaling law is obtained. These scaling laws imply that as the density of the matter increases the effective quantities in medium scale down.

We have shown how a slight modification of the Lagrangian resolves the  $\omega$  problem. However, in modifying the Lagrangian we have taken into account only the phenomenological side of the problem. Multiplying the Wess-Zumino term by the factor  $(\chi/f_\chi)^n$  has no sound theoretical support. It breaks explicitly the scale invariance of the Lagrangian. Recall that the dilaton field was introduced into the model to respect scale symmetry. Furthermore, we don't have any special reason for choosing  $n = 3$ , except that it works well. Recently, a more fundamental explanation for the behavior in Eq.(1.51) has been found.<sup>d</sup>

## 1.6. Conclusions

In trying to understand what happens to hadrons under extreme conditions, it is necessary that the theory adopted for the description be consistent with QCD. In terms of effective theories this means that they should match to QCD at a scale close

<sup>d</sup>Private communication by M. Rho on work in progress by H.K. Lee and M. Rho.

to the chiral scale  $\Lambda_\chi \sim 4\pi f_\pi \sim 1$  GeV. It has been shown that this matching can be effectuated in the framework of hidden local symmetry (HLS) and leads to what is called ‘vector manifestation’ (VM)<sup>23</sup> which provides a theoretical support for a low-energy effective field theory for hadrons and which gives, in the chiral limit, an elegant and unambiguous prediction of the behavior of light-quark hadrons at high temperature and/or at high density. Following the indications of the HLS theory, we have described a Skyrme model in which the dilaton field  $\chi$ , whose role in dense matter was first pointed out by Brown and Rho,<sup>49</sup> and the vector meson fields  $\rho$  and  $\omega$  were incorporated into the Skyrme Lagrangian to construct dense skyrmion matter.

We have presented an approach to hadronic physics based on Skyrme’s philosophy, namely that baryons are solitons of a theory described in terms of meson fields, which can be justified from QCD in the large  $N_c$  expansion. We have adopted the basic principles of effective field theory. Given a certain energy domain we describe the dynamics by a Lagrangian defined in terms of the mesonic degrees of freedom active in that domain, we thereafter implement the symmetries of QCD and VM, and describe the baryonic sectors as topological winding number sectors and solve in these sectors the equations derived from the Lagrangian with the appropriate boundary conditions for the sector. In this way one can get all of Nuclear Physics out of a single Lagrangian. We have studied the B=1 sector to obtain the properties of the single skyrmion, the B=2 sector to understand the interaction between skyrmions, and our main effort has been the study skyrmion matter, as a model for hadronic matter, investigating its behavior at finite density and temperature and the description of meson properties in that dense medium.

Skyrme models have been proven successful in describing nuclei, the nucleon-nucleon interaction and pion-nucleon interactions. It turns out that Skyrme models also represent a nice tool for understanding low density cold hadronic matter and the behavior of the mesons in particular the pion inside matter. We have shown in here that when hadronic matter is compressed and/or heated Skyrme models provide useful information on the chiral phase transitions. Skyrmion matter is realized as a crystal and we have seen that at low densities it is an FCC crystal made of skyrmions. The phase transition occurs when the FCC crystal transforms into a half skyrmion CC one. In our study we have discovered the crucial role of the scale dilaton in describing the expected phase transition towards a chiral symmetry restored phase. We have also noticed the peculiar behavior of the  $\omega$  associated to its direct coupling to the baryon number current and we have resolved the problem by naturally scaling the coupling constant using the scale dilaton.

Another aspect of our review has been the study of the properties of elementary mesons in the medium, in particular those involved in the model, the pion and the dilaton. Moreover we have described how their properties change when we move from one phase to another.

A description of the chiral restoration phase transition in the temperature-

density plane has been presented, whose main ingredient is that the dominant scenario is the absorption of heat by the fluctuating pions in the background of crystal skyrmion matter. This description leads to a phase transition whose dynamical structure is parameter independent and whose shape resembles much the conventional confinement/deconfinement phase transition. We obtain, for parameter values close the conventional ones, the expected critical temperatures and densities.

For clarity, the presentation has been linear, in the sense, that given the Lagrangian we have described its phenomenology, and have made no effort to interpret the mechanisms involved and the results obtained from QCD. In this way we have taken a ‘bottom up’ approach: the effective theory represents confined QCD and it should explain the hadronic phenomenology in its domain of validity.

The main result of our calculation is the realization that phase transition scenario is not as simple as initially thought but contains many features which make interesting and phenomenologically appealing. It is now time to try to collect ideas based on fundamental developments and see how our effective theory and the principles that guide it realize these ideas. In this line of thought, it is exciting to have unveiled scenarios near the phase transition of unexpected interesting phenomenology in line with recent proposals.<sup>66,67</sup>

### Acknowledgements

We would like to thank our long time collaborators Dong-Pil Min and Hee-Jung Lee whose work is reflected in these pages and who have contributed greatly to the effort. We owe inspiration and gratitude to Mannque Rho, who during many years has been a motivating force behind our research. Skyrmion physics had a boom in the late 80’s and thereafter only a few groups have maintained this activity obtaining very beautiful results, which however, have hardly influenced the community. We hope that this book contributes to make skyrmion physics more widely appreciated. Byung-Yoon Park thanks the members of Departamento de Física Teórica of the University of Valencia for their hospitality. Byung-Yoon Park and Vicente Vento were supported by grant FPA2007-65748-C02-01 from Ministerio de Ciencia e Innovación.

### References

1. J.-e. Alam, S. Chattopadhyay, T. Nayak, B. Sinha, and Y. P. Viyogi, Quark Matter 2008, *J. Phys.* **G35**, 100301, (2008).
2. T. H. R. Skyrme, A Nonlinear field theory, *Proc. Roy. Soc. Lond.* **A260**, 127, (1961).
3. T. H. R. Skyrme, A Unified Field Theory of Mesons and Baryons, *Nucl. Phys.* **31**, 556, (1962).
4. F. Karsch, Recent lattice results on finite temperature and density QCD, part II, *PoS. LAT2007*, 015, (2007).
5. M. Fromm and P. de Forcrand, Revisiting strong coupling QCD at finite temperature and baryon density. (2008).

6. G. 't Hooft, A Planar Diagram Theory For Strong Interactions, *Nucl. Phys.* **B72**, 461, (1974).
7. H.-J. Lee, B.-Y. Park, D.-P. Min, M. Rho, and V. Vento, A unified approach to high density: Pion fluctuations in skyrmion matter, *Nucl. Phys.* **A723**, 427, (2003).
8. B.-Y. Park, M. Rho, and V. Vento, Vector mesons and dense skyrmion matter, *Nucl. Phys.* **A736**, 129, (2004).
9. B.-Y. Park, M. Rho, and V. Vento, The Role of the Dilaton in Dense Skyrmion Matter, *Nucl. Phys.* **A807**, 28, (2008).
10. H.-J. Lee, B.-Y. Park, M. Rho, and V. Vento, Sliding vacua in dense skyrmion matter, *Nucl. Phys.* **A726**, 69, (2003).
11. H.-J. Lee, B.-Y. Park, M. Rho, and V. Vento, The Pion Velocity in Dense Skyrmion Matter, *Nucl. Phys.* **A741**, 161, (2004).
12. A. C. Kalloniatis, J. D. Carroll, and B.-Y. Park, Neutral pion decay into nu anti-nu in dense skyrmion matter, *Phys. Rev.* **D71**, 114001, (2005).
13. A. C. Kalloniatis and B.-Y. Park, Neutral pion decay in dense skyrmion matter, *Phys. Rev.* **D71**, 034010, (2005).
14. B.-Y. Park, H.-J. Lee, and V. Vento, Skyrmions at finite density and temperature: the chiral phase transition. (2008).
15. E. Witten, Current Algebra, Baryons, and Quark Confinement, *Nucl. Phys.* **B223**, 433, (1983).
16. G. S. Adkins, C. R. Nappi, and E. Witten, Static Properties of Nucleons in the Skyrme Model, *Nucl. Phys.* **B228**, 552, (1983).
17. A. D. Jackson and M. Rho, Baryons as Chiral Solitons, *Phys. Rev. Lett.* **51**, 751, (1983).
18. E. Witten, Global Aspects of Current Algebra, *Nucl. Phys.* **B223**, 422, (1983).
19. S. Weinberg, Phenomenological Lagrangians, *Physica.* **A96**, 327, (1979).
20. A. A. Migdal and M. A. Shifman, Dilaton Effective Lagrangian in Gluodynamics, *Phys. Lett.* **B114**, 445, (1982).
21. J. R. Ellis and J. Lanik, Is scalar gluonium observable?, *Phys. Lett.* **B150**, 289, (1985).
22. M. Bando, T. Kugo, and K. Yamawaki, Nonlinear Realization and Hidden Local Symmetries, *Phys. Rept.* **164**, 217, (1988).
23. M. Harada and K. Yamawaki, Hidden local symmetry at loop: A new perspective of composite gauge boson and chiral phase transition, *Phys. Rept.* **381**, 1, (2003).
24. I. R. Klebanov, Nuclear matter in the skyrme model, *Nucl. Phys.* **B262**, 133, (1985).
25. A. S. Goldhaber and N. S. Manton, Maximal symmetry of the skyrme crystal, *Phys. Lett.* **B198**, 231, (1987).
26. A. D. Jackson and J. J. M. Verbaarschot, Phase structure of the skyrme model, *Nucl. Phys.* **A484**, 419, (1988).
27. Z. Tesanovic, O. Vafek, and M. Franz, Chiral symmetry breaking and phase fluctuations: A QED-3 theory of the pseudogap state in cuprate superconductors, *Phys. Rev.* **B65**, 180511, (2002).
28. G. Kaelbermann, Nuclei as skyrmion fluids, *Nucl. Phys.* **A633**, 331, (1998).
29. O. Schwindt and N. R. Walet, Soliton systems at finite temperatures and finite densities. (2002).
30. I. Zahed and G. E. Brown, The Skyrme Model, *Phys. Rept.* **142**, 1, (1986).
31. A. Jackson, A. D. Jackson, and V. Pasquier, The Skyrmion-Skyrmion Interaction, *Nucl. Phys.* **A432**, 567, (1985).
32. B. Schwesinger, H. Weigel, G. Holzwarth, and A. Hayashi, The skyrme soliton in pion, vector and scalar meson fields: pi n scattering and photoproduction, *Phys. Rept.* **173**, 173, (1989).

33. L. Castillejo, P. S. J. Jones, A. D. Jackson, J. J. M. Verbaarschot, and A. Jackson, Dense Skyrmion Systems, *Nucl. Phys.* **A501**, 801, (1989).
34. M. Kugler and S. Shtrikman, A new skyrmion crystal, *Phys. Lett.* **B208**, 491, (1988).
35. N. S. Manton and P. M. Sutcliffe, Skyrme crystal from a twisted instanton on a four torus, *Phys. Lett.* **B342**, 196, (1995).
36. M. Kutschera, C. J. Pethick, and D. G. Ravenhall, Dense matter in the chiral soliton model, *Phys. Rev. Lett.* **53**, 1041, (1984).
37. M. Kugler and S. Shtrikman, Skyrmion crystals and their symmetries, *Phys. Rev.* **D40**, 3421, (1989).
38. H. Forkel et al., Chiral symmetry restoration and the skyrme model, *Nucl. Phys.* **A504**, 818, (1989).
39. M. F. Atiyah and N. S. Manton, Skyrmions from Instantons, *Phys. Lett.* **B222**, 438, (1989).
40. M. F. Atiyah and N. S. Manton, Geometry and kinematics of two skyrmions, *Commun. Math. Phys.* **153**, 391, (1993).
41. R. A. Leese and N. S. Manton, Stable instanton generated Skyrme fields with baryon numbers three and four, *Nucl. Phys.* **A572**, 575, (1994).
42. N. R. Walet, Quantising the B=2 and B=3 Skyrmion systems, *Nucl. Phys.* **A606**, 429, (1996).
43. B.-Y. Park, D.-P. Min, M. Rho, and V. Vento, Atiyah-Manton approach to Skyrmion matter, *Nucl. Phys.* **A707**, 381, (2002).
44. R. Jackiw, Quantum meaning of classical field theory, *Rev. Mod. Phys.* **49**(3), 681.
45. S. Saito, T. Otofujii, and M. Yasino, Pion Fluctuations about the Skyrmion, *Prog. Theor. Phys.* **75**, 68, (1986).
46. H. Yabu, F. Myhrer, and K. Kubodera, Meson condensation in dense matter revisited, *Phys. Rev.* **D50**, 3549, (1994).
47. V. Thorsson and A. Wirzba, S-wave Meson-Nucleon Interactions and the Meson Mass in Nuclear Matter from Chiral Effective Lagrangians, *Nucl. Phys.* **A589**, 633, (1995).
48. W. R. Gibbs and W. B. Kaufmann, The Contribution of the Quark Condensate to the pi N Sigma Term, *nucl-th/0301095*. (2003).
49. G. E. Brown and M. Rho, Scaling effective Lagrangians in a dense medium, *Phys. Rev. Lett.* **66**, 2720, (1991).
50. G. E. Brown, A. D. Jackson, M. Rho, and V. Vento, The nucleon as a topological chiral soliton, *Phys. Lett.* **B140**, 285, (1984).
51. R. J. Furnstahl, H.-B. Tang, and B. D. Serot, Vacuum contributions in a chiral effective Lagrangian for nuclei, *Phys. Rev.* **C52**, 1368, (1995).
52. C. Song, G. E. Brown, D.-P. Min, and M. Rho, Fluctuations in 'Brown-Rho scaled' chiral Lagrangians, *Phys. Rev.* **C56**, 2244, (1997).
53. H. Reinhardt and B. V. Dang, Modified Skyrme Model with correct QCD scaling behavior on S3, *Phys. Rev.* **D38**, 2881, (1988).
54. K. Zarembo, Possible pseudogap phase in qcd, *JETP Lett.* **75**, 59, (2002).
55. T. Hatsuda and T. Kunihiro, The sigma-meson and pi pi correlation in hot/dense medium: Soft modes for chiral transition in QCD. (2001).
56. H. Fujii, Scalar density fluctuation at critical end point in NJL model, *Phys. Rev.* **D67**, 094018, (2003).
57. R. D. Pisarski and M. Tytgat, Propagation of Cool Pions, *Phys. Rev.* **D54**, 2989, (1996).
58. H. Leutwyler, Nonrelativistic effective Lagrangians, *Phys. Rev.* **D49**, 3033, (1994).
59. M. Kirchbach and A. Wirzba, In-medium chiral perturbation theory and pion weak decay in the presence of background matter, *Nucl. Phys.* **A616**, 648, (1997).

60. D. T. Son and M. A. Stephanov, Real-time pion propagation in finite-temperature QCD, *Phys. Rev.* **D66**, 076011, (2002).
61. A. Bochkevich and J. I. Kapusta, Chiral symmetry at finite temperature: linear vs nonlinear  $\sigma$ -models, *Phys. Rev.* **D54**, 4066, (1996).
62. I. Arsene et al., Quark-gluon plasma and color glass condensate at RHIC? The perspective from the BRAHMS experiment, *Nuclear Physics A.* **757**(1-2), 1.
63. U. G. Meissner, Low-energy hadron physics from effective chiral lagrangians with vector mesons, *Phys. Rept.* **161**, 213, (1988).
64. B. D. Serot and J. D. Walecka, The relativistic nuclear many body problem, *Adv. Nucl. Phys.* **16**, 1, (1986).
65. U.-G. Meissner, A. Rakhimov, and U. T. Yakhshiev, The nucleon nucleon interaction and properties of the nucleon in a pi rho omega soliton model including a dilaton field with anomalous dimension, *Phys. Lett.* **B473**, 200, (2000).
66. L. McLerran, Quarkyonic Matter and the Phase Diagram of QCD. (2008).
67. L. McLerran and R. D. Pisarski, Phases of Cold, Dense Quarks at Large  $N_c$ , *Nucl. Phys.* **A796**, 83, (2007).